

SCIENTIFIC REPORTS



OPEN

Self-assembly of c-myc DNA promoted by a single enantiomer ruthenium complex as a potential nuclear targeting gene carrier

Qiong Wu¹, Wenjie Mei¹, Kangdi Zheng² & Yang Ding¹

Gene therapy has long been limited in the clinic, due in part to the lack of safety and efficacy of the gene carrier. Herein, a single enantiomer ruthenium(II) complex, Λ -[Ru(bpy)₂(*p*-BEPIP)](ClO₄)₂ (Λ -RM0627, bpy = 4,4'-bipyridine, *p*-BEPIP = 2-(4-phenylacetylenophenyl)imidazole [4,5*f*][1, 10] phenanthroline), has been synthesized and investigated as a potential gene carrier that targets the nucleus. In this report, it is shown that Λ -RM0627 promotes self-assembly of *c-myc* DNA to form a nanowire structure. Further studies showed that the nano-assembly of *c-myc* DNA that induced Λ -RM0627 could be efficiently taken up and enriched in the nuclei of HepG2 cells. After treatment of the nano-assembly of *c-myc* DNA with Λ -RM0627, over-expression of *c-myc* in HepG2 cells was observed. In summary, Λ -RM0627 played a key role in the transfer and release of *c-myc* into cells, which strongly indicates Λ -RM0627 as a potent carrier of *c-myc* DNA that targets the nucleus of tumor cells.

Gene therapy, which encompasses an extensive variety of treatment types, all of which use genetic material to modify damaged cells in an attempt to effect a cure, has long been investigated and considered a promising approach to treat cancer^{1–3}. Significant progress has been made in gene therapy, particularly at the animal level, and considerable effort has been exerted to increase the efficiency and safety of this approach^{4,5}. It is also worth mentioning that the cell nucleus is the major site of DNA replication and transcription, which is the essential target of the gene carrier to affect the functional expression of genes in the cell⁶. Thus, if one gene carrier can target the transfection of a given gene into the nucleus, this might enhance both the transfection efficiency and the stability of gene expression.

Generally, this technology is designed to kill tumor cells directly through introduction of genes called suicide genes; for example, siRNA, miRNA, and mRNA that are targeted to tumor cells^{7,8}. Moreover, the inhibition of *c-myc* oncogenic expression can inhibit the proliferation of tumor cells, which is significant because of the critical role played by *c-myc* in regulating the proliferation, division, and metabolism of cells⁹. More importantly, *c-myc* is one of the most crucial transcription factors that regulates the induction of pluripotent stem cells (iPSCs), in which transient expression of the *c-Myc* transgene plays an important role in the resultant iPSCs^{10,11}. However, there remain quite significant limitations in the clinical application of not only common gene delivery methods (e.g., nano-liposomes and electroporation), but also the use of retroviral or lentiviral vector systems, due to the lack of an efficient and safe vector system for gene delivery^{12–15}.

To date, considerable effort has been exerted in the design of an efficient gene delivery system. Moreover, non-viral gene vectors, like polymers, liposomes, peptides, chitosan, and nanoparticles, have been extensively investigated. Recently, inorganic materials, such as ultra-small (~2 nm) gold (Au) nanoparticles, have been used to deliver triplex oligonucleotides into the nuclei of cells¹⁶. Furthermore, transition metal complexes, particularly ruthenium (II) complexes, have been utilized to condense and deliver DNA into cells because of their strong fluorescence, high DNA binding affinity, and low toxicity in biological environments^{17–20}. For example, Kumbhar *et al.*, revealed two water-soluble ruthenium (II) polypyridyl complexes as carriers for DNA delivery²¹. Chao *et al.* also developed a luminescent tetranuclear ruthenium (II) complex that served as a tracking non-viral gene vector^{22–25}.

¹School of Pharmacy, Guangdong Pharmaceutical University, Guangzhou 510006, China. ²Traditional Chinese Medicine College, Guangdong Pharmaceutical University, Guangzhou 510006, China. Correspondence and requests for materials should be addressed to W.M. (email: wenjiemei@126.com)

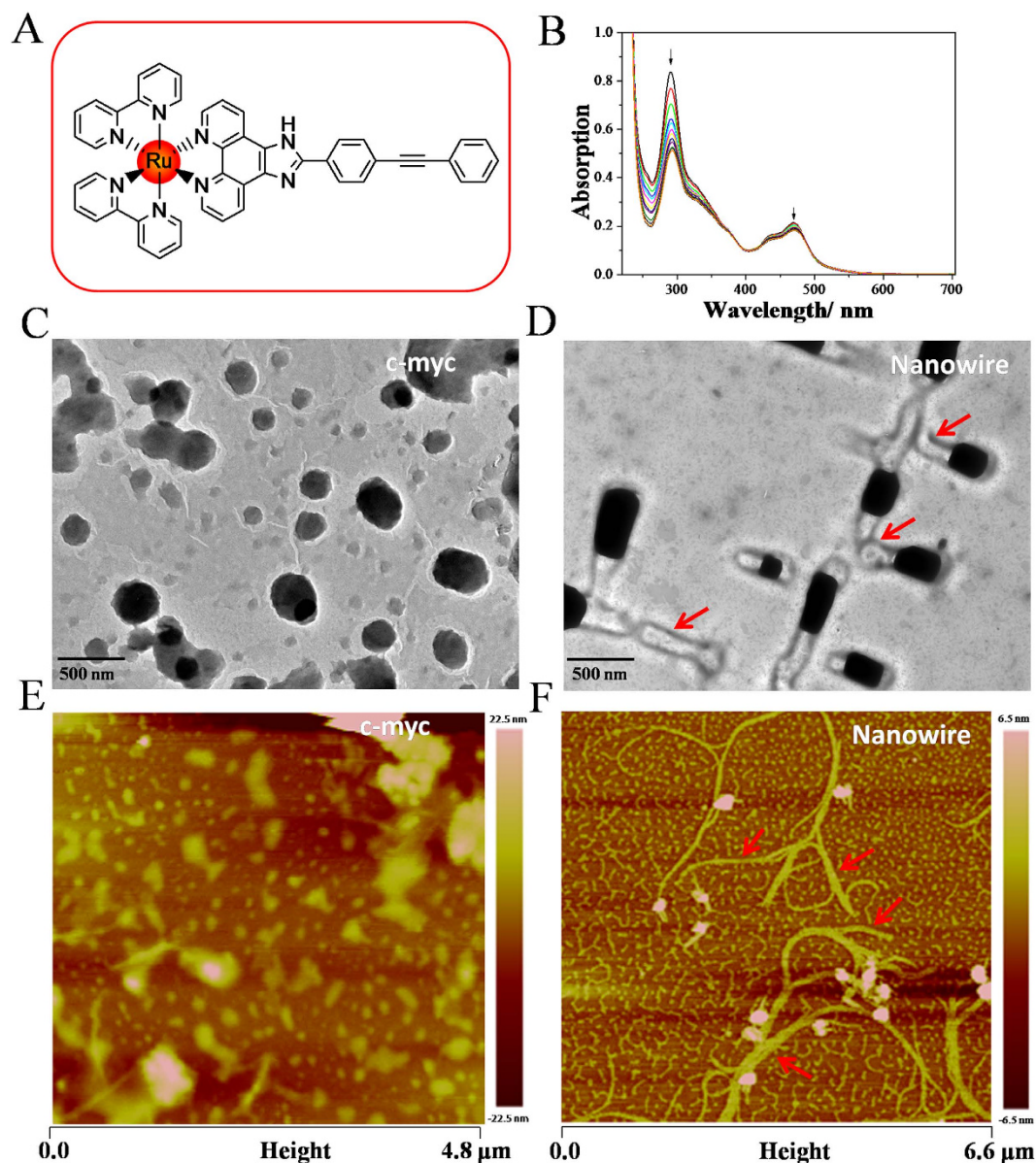


Figure 1. Self-assembly of *c-myc* G-quadruplex DNA induced by ruthenium complex Δ -RM0627. (A) Shows the molecular structure of the a single enantiomer ruthenium (II) complex of Δ -RM0627. (B) The electronic spectra of Δ -RM0627 (20 μ M, and 3 mL) were determined following the addition of the *c-myc* G-quadruplex DNA (100 μ M) at a rate of 2 μ L every 5 minutes. ($[c-myc] = 0.0667 \mu$ M, $n = 0, 1, 2, 3, \dots 9$, etc.) in Tris-HCl buffer (pH 7.2, containing 100 mM KCl). (C) TEM image of free *c-myc* DNA (5 μ M) in Tris-HCl KCl solution (pH 7.2) that was air-dried. (D) TEM image of *c-myc* DNA (5 μ M) self-assembled into nanostructures in the presence of Δ -RM0627 (5 μ M) in Tris-HCl KCl buffer (pH 7.2) and air-dried. (E) AFM image of *c-myc* DNA (5 μ M) in the absence of Δ -RM0627. (F) AFM image of the nano-assembly of *c-myc* DNA (5 μ M) in the presence of Δ -RM0627.

To the best of our knowledge, ruthenium (II) complexes can bind to double-stranded DNA molecules in the intercalating, groove binding, and electrostatic binding modes. Furthermore, the studies by Ji *et al.* showed that ruthenium (II) complexes can bind and stabilize the G-quadruplex DNA structure^{26,27}. Furthermore, Qu *et al.* found that a zinc-finger-like a single enantiomer metallo-supramolecular complex of NiP, exhibited a single enantiomer selectivity to cancer cells, owing to the target G-quadruplex DNA of telomeres²⁸.

Recently, Tan *et al.* achieved many remarkable results in the field of DNA nano-assembly, which might be applied to potential gene carriers, drug delivery systems, and gene-silencing therapy and cellular imaging^{3,29–31}. By contrast, evidence has previously showed that the guanine-rich sequence of the *c-myc* promoter forms G-quadruplex structures because of three or four guanine bases that are associated in a cyclic array via Hoogsteen hydrogen bonding arrangements^{32,33}. Studies in our laboratory showed that ruthenium (II) complexes can also facilitate stability of the *c-myc* G-quadruplex DNA^{34,35}.

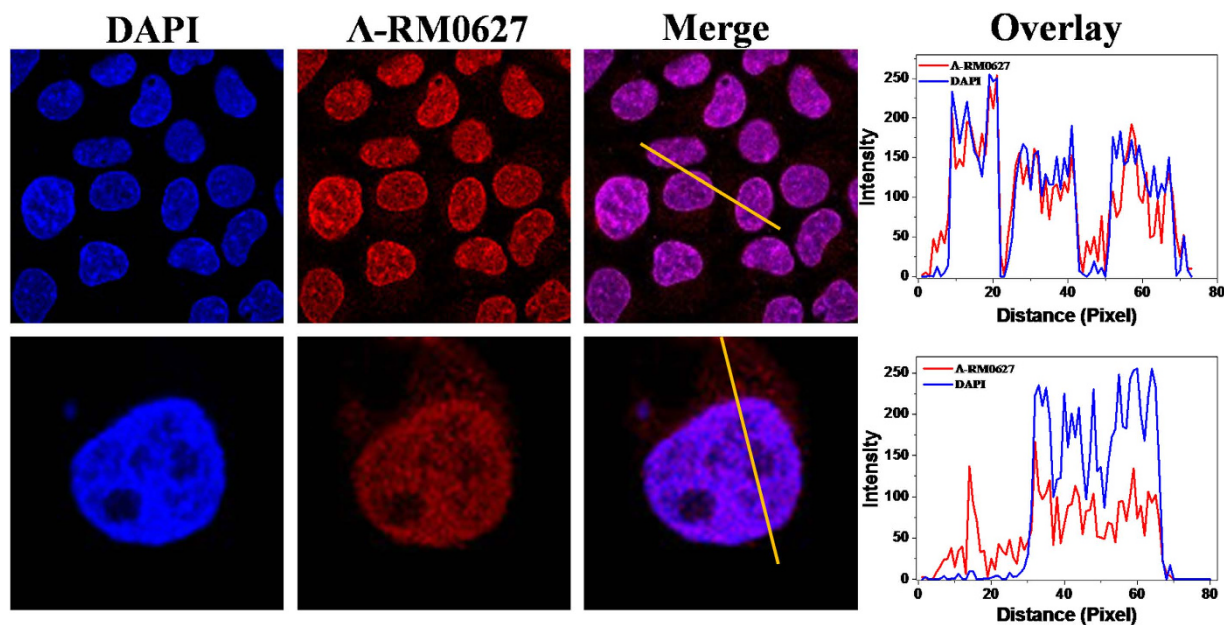


Figure 2. The distribution and localization of ruthenium complex Λ -RM0627. Confocal laser scanning microscopic images of the HepG2 cell nucleus in the presence of Λ -RM0627 ($5\ \mu\text{M}$) treatment for 2 h. The overlay data was analyzed by Image Pro Plus.

With these findings in mind, we hypothesized that a single enantiomer polypyridine ruthenium (II) complex can bind to *c-myc* G-quadruplex DNA and promote the self-assembly of the *c-myc* G-quadruplex DNA. The self-assembled particles carry the DNA into the nuclei of living cells, following which, the DNA is released and functionally expressed as normal. It is anticipated that this approach will help develop a new potential gene carrier system, which might significantly promote the development of gene therapy.

Results

Interaction between *c-myc* G-quadruplex DNA with Λ -RM0627. A single enantiomer ruthenium (II) complex with 2-(4-phenylacetylenophenyl)imidazole[4,5*f*][1,10]phenanthroline (*p*-BEPIP), Λ -[Ru(*bpy*)₂(*p*-BEPIP)](ClO₄)₂ (Λ -RM0627, *bpy* = 4,4'-bipyridine) (Fig. 1A), was synthesized in the presence of Pd-Cu catalyst by using microwave-assisted synthesis technology. The binding properties of this complex with *c-myc* G-quadruplex DNA was confirmed by electronic spectra experiments, which is a classic and common method to evaluate the interactions of small molecules with biological macromolecules. According to the electronic spectra experiments, it's revealed that Λ -RM0627 exhibited strong binding affinity to *c-myc* G4-DNA. This was confirmed by the hypochromism in the electronic absorption of Λ -RM0627 in the presence of *c-myc* G4-DNA. In general, there are characteristic MLCT (metal to ligand charge transfer) absorption in the range of 400–550 nm with a maximum absorption at a wavelength of 470 nm, the IL (i.e., the intraligand charge transfer) absorption in the range of 250–300 nm with a maximum at 290 nm, and a shoulder absorption was observed at a wavelength of 370 nm that could be attributed to the LMCT (i.e., the ligand to metal charge transfer) transition were observed in the electronic spectra of Λ -RM0627 in Tris-HCl buffer (pH 7.2). After G4-DNA was added into the solution, the hypochromism at the MLCT and IL absorption was 14.6 and 38.9%, respectively (Fig. 1B). These data demonstrated that this complexes bind to the *c-myc* G4-DNA with a high affinity³⁶.

DNA self-assembly promoted by Λ -RM0627. The self-assembly of the *c-myc* G-quadruplex DNA induced by Λ -RM0627 was confirmed by TEM. We observed that anomalous spherical and compact DNA condensates with diameters of approximately 250 nm were formed by the free-*c-myc* G-quadruplex DNA (Fig. 1C). For the *c-myc* G-quadruplex DNA that was incubated with Λ -RM0627, a typical pipeline-like structure with a diameter of approximately 200 nm was observed, indicating that DNA was self-assembled into a nanowire structure in the presence of Λ -RM0627 (Fig. 1D)³⁶. Notably, a black area was observed at the terminal and connecting junction of the DNA nanowire²⁴.

Atomic force microscopy (AFM) provided additional insights into the self-assembly of the *c-myc* G-quadruplex DNA that was induced by Λ -RM0627. We observed that free-*c-myc* DNA formed a number of irregular and spherical DNA particles with sizes of about 50–500 nm and had a height of approximately 22.5 nm (Fig. 1E), which corresponded with the findings obtained by TEM. Thus, we observed a perfect nanowire structure of self-assembled *c-myc* DNA that was promoted by Λ -RM0627. The assembled nanowire had a width of about 25–200 nm and a height of approximately 6.5 nm (Fig. 1F), a typical thickness previously reported for nanowire structures^{36–39}. Moreover, we observed many red points at the terminal and conjunction of the nanowire, which may be the complex Λ -RM0627 confined in the G-quadruplex conformation of DNA²⁴.

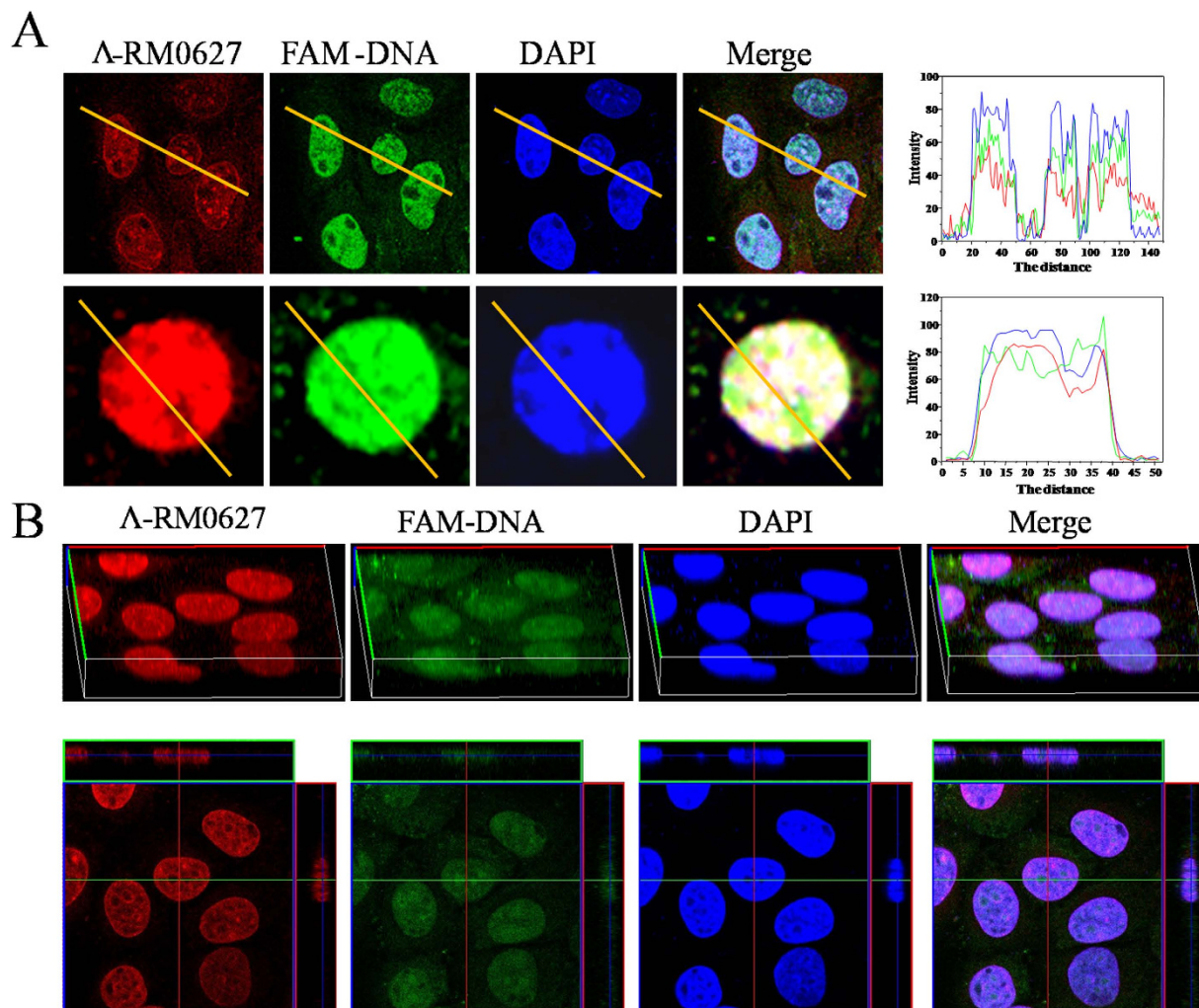


Figure 3. The distribution and localization of the nano-assembly. (A) Confocal laser scanning microscopic image of the HepG2 cellular nucleus in the presence of FAM-*c-myc* (5 μ M) + Λ -RM0627 (5 μ M). (B) A 3D-tomoscan image of the HepG2 nucleus in the presence of FITC-*c-myc* (5 μ M) + Λ -RM0627 (5 μ M). Red staining shows the a single enantiomer ruthenium (II) complex Λ -RM0627 green staining shows the FAM tagged *c-myc* G-quadruplex DNA and blue staining shows DAPI nuclear counter-staining. The overlay data was analyzed by Image Pro Plus.

Distribution of a single enantiomer ruthenium complex Λ -RM0627. This study tested the ability of cellular uptake of a single enantiomer ruthenium complex Λ -RM0627 by HepG2 cells. The a single enantiomer ruthenium (II) complex Λ -RM0627 (5 μ M) was incubated for 2 h, and it was completely absorbed and localized in the nuclei of HepG2 cells (Fig. 2). Interestingly, co-staining with the cyanine dye DAPI, a general nucleic acid stain, shows a clear superposition in localization on nucleus^{40,41}. In an enlarged image, one can see the emission of Λ -RM0627 (red fluorescence) that was merged to blue fluorescence with an overlay rate near 100 percent. These results indicated that complex Λ -RM0627 can immediately enter the nucleus.

Localization of nano-assembly. Given their massive size and low penetrating ability, free DNA cannot enter living cells, which was confirmed in our experiments, wherein the *c-myc* G-quadruplex DNA itself could not be absorbed by HepG2 cells and instead aggregated to the cell surface (Supplementary Fig. 3)⁴². Thus, the FAM (green)-tagged *c-myc* G-quadruplex DNA was used to indicate the location of DNA in cells. After treatment with Λ -RM0627, the nanowire self-assembled FAM-*c-myc* G-quadruplex DNA was added to HepG2 cells in fresh DMEM that was supplemented with 10% FBS and incubated with cells for 6 h (Supplementary Fig. 2A). The cellular uptake of DNA was directly observed under confocal laser fluorescence microscopy, and the nuclei of HepG2 cells were stained with 4',6-diamidino-2-phenylindole (DAPI; blue)^{17,18,22}.

We observed that the bright green fluorescence (FAM-*c-myc* G-quadruplex DNA) and red fluorescence (Λ -RM0627) were almost at the same site and completely overlaid the blue fluorescence, indicating that the *c-myc* G-quadruplex DNA was successfully absorbed by the cells and localized in the nuclei of the cells (Fig. 3A). In the enlarged image, three-color fluorescence was localized in the same position⁴³. Notably, the overlap ratio of DNA, Λ -RM0627, and DAPI was approximately 100 percent (Fig. 3B). In addition, in three-dimensional

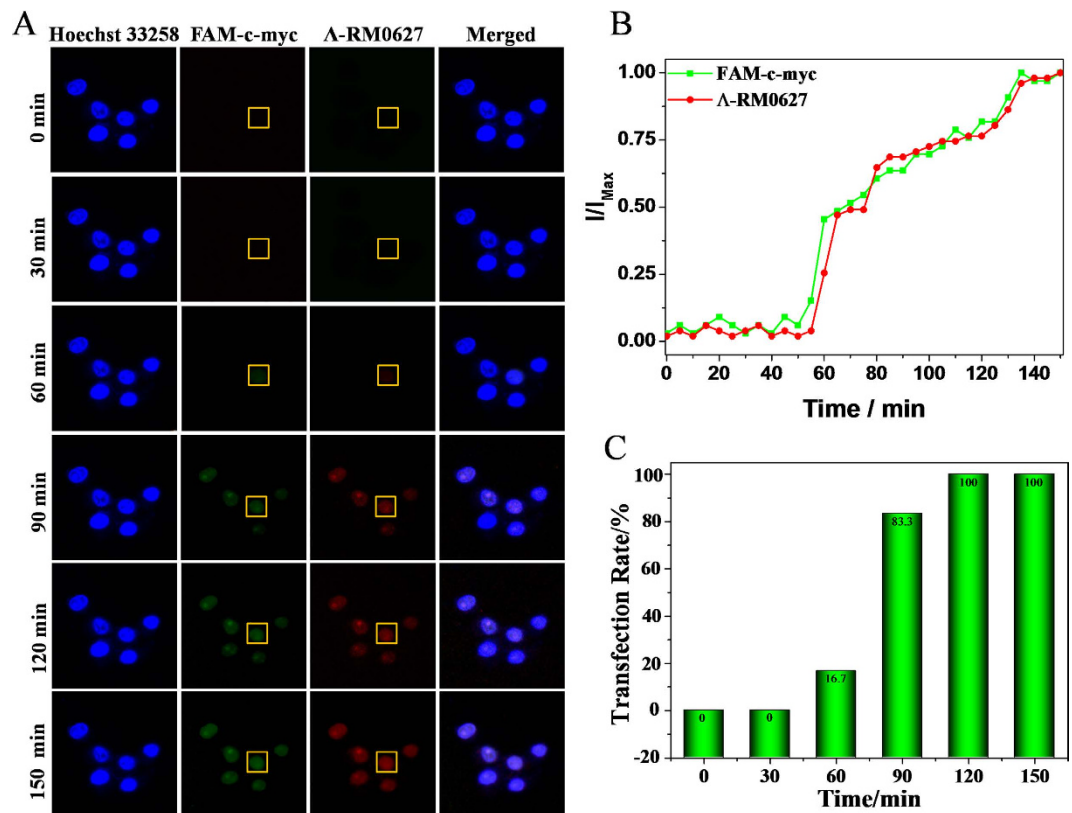


Figure 4. The cellular uptake of the nano-assembly. (A) Real-time fluorescence images of HepG2 cells treated with *c-myc* G-quadruplex DNA + Δ -RM0627 (5 μ M) for 0, 30, 60, 90, 120, and 150 min. (B) Merged position of green and red fluorescence with time. I_{Max} is the fluorescence seen at 150 min. (C) Time-dependent cellular uptake of the *c-myc* G-quadruplex DNA + Δ -RM0627 in HepG2 cells.

tomoscan imaging, the green fluorescence filled the entire nucleus and was matched to the staining pattern seen for Δ -RM0627 and DAPI. This finding indicated that the Δ -RM0627 complex could carry FAM-*c-myc* DNA into the nuclei of tumor cells.

Real-time observation of cellular uptake of nano-assembly. To further clarify the possibility of Δ -RM0627 behaving as a potential fluorescence vector to carry specific genes into living cell nuclei, real-time fluorescence observations verified the cellular uptake of the *c-myc* G-quadruplex DNA nanowire that was induced by Δ -RM0627 in living HepG2 cells. The nuclei of HepG2 cells were stained blue by Hoechst 33258 (a typical vital nuclear dye). The DNA particles were then added to the HepG2 cells in DMEM containing 10% FBS. Images were captured every 5 min. After 60 min of incubation, the green fluorescence ascribed to the FAM-*c-myc* G-quadruplex DNA was observed in the nuclei of HepG2 cells. The intensity of green fluorescence and the number of green fluorescently stained cells gradually increased with time (Fig. 4A). Notably, the characterized red fluorescence of Δ -RM0627 was observed at the same site as *c-myc* G-quadruplex DNA in the nuclei.

The time-dependent changes in fluorescence intensity completely corresponded with that of the *c-myc* G-quadruplex DNA during the entire process (Fig. 4B), which indicated that DNA was carried into the nuclei of living cells by Δ -RM0627. After 120 min, the intensity of green fluorescence peaked, and the cellular uptake reached approximately 100 percent (Fig. 4C). These results indicated that the nano-assembled *c-myc* G-quadruplex DNA could transfect cells efficiently as compared with Lipofectamine 2000, which is a classic gene carrier reagent that transfects FAM-*c-myc* G-quadruplex DNA into cells in approximately 6 h and to some extent induces cellular damage (Supplementary Fig. 5)⁴⁴. Moreover, this finding inspired us to develop Δ -RM0627 as an efficient carrier to deliver DNA into the nuclei of living cells for future clinical applications with the aim of accelerating and promoting gene therapy.

The expression of the nano-assembly. To evaluate the feasibility and effectiveness of this system, the RT-qPCR experiment was completed to define the release and transfection of the *c-myc* G-quadruplex nano-assembly that was induced by Δ -RM0627 in HepG2 cells. Next, data that was obtained by RT-qPCR showed that the ruthenium complex delivered *c-myc* into living cells and enabled normal expression of the *c-myc* gene. With increasing concentrations of the nano-assembly, the expression of the *c-myc* gene was clearly enhanced in HepG2 cells. When the nanoassembly system concentration was 5 μ M, the expression of the *c-myc* gene was increased by approximately 17.5 percent as compared to 10.9 percent of Lipofectamine 2000, in which the results

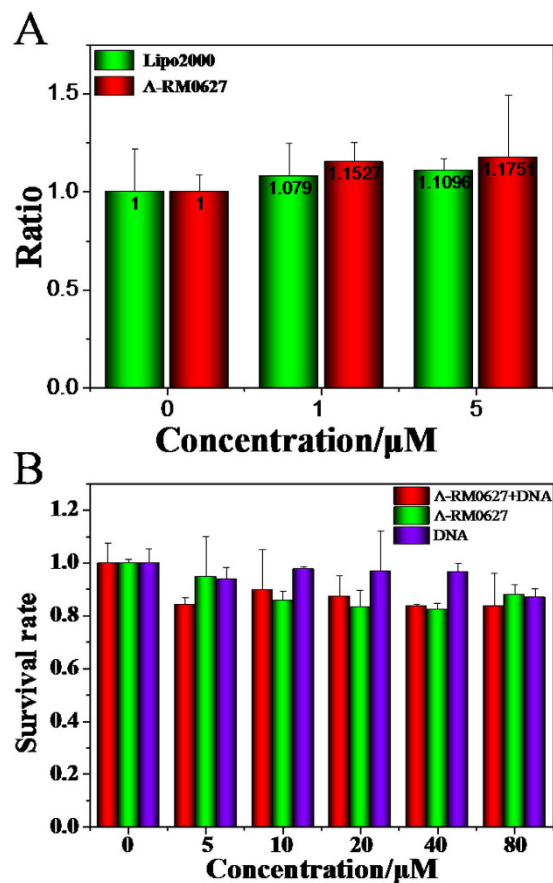


Figure 5. Expression of the *c-myc* gene and the toxicity of the *c-myc* nano-assembly induced by Λ -RM0627. (A) Regulation of the expression of *c-myc* DNA delivered by Lipofectamine 2000 and ruthenium complex Λ -RM0627 at the RNA level. [DNA/Lipofectamine 2000] = 1 $\mu\text{g}/10 \mu\text{L}$; [DNA]: [Λ -RM0627] = 1:1 [DNA] = (0, 1 and 5 μM). (B) The cytotoxicity of the a single enantiomer ruthenium (II) complex Λ -RM0627, free *c-myc* DNA and Λ -RM0627 + *c-myc* DNA is shown. All data were obtained from three independent experiments and were presented as the mean \pm SD. $P < 0.05$ vs untreated control. Error bars represent the mean standard deviation.

indicated that the nano-assembly of *c-myc* DNA could not only enter living cells quickly, but could also release and express *c-myc* normally⁴⁵. These results were agreement with the researches of Chao group, which the ruthenium complex can deliver the DNA into the cells and the gene can express normally in cells²⁴.

The cytotoxicity of the nano-assembly. The cytotoxicity of Λ -RM0627, free *c-myc* DNA and the nano-assembly were evaluated by MTT with HepG2 cells, respectively. According to the MTT assay, it was found that Λ -RM0627 and free *c-myc* DNA displayed no significant inhibitory effect on growth, in which about 90 percent of cells remained viable (Fig. 5B). Moreover, these results indicated that the nano-assembly exhibited low cytotoxicity against HepG2 cells, in which the cell survival rate still exceeded 80 percent when the concentration reached 80 μM ¹⁷.

Discussion

In this regard, a novel approach has been constructed to develop a potent gene carrier system to target the nucleus of tumor cells. The current technology has focused on the nanowire structure formed from the self-assembly of *c-myc* DNA that was promoted by a novel a single enantiomer ruthenium (II) complex, Λ -RM0627. The nanowire of the assembled *c-myc* G-quadruplex DNA was rapidly absorbed and localized to the nucleus, and consequently, the expression of the *c-myc* gene was up-regulated. To our knowledge, this study is the first attempt to utilize a single enantiomer ruthenium (II) complexes to carry DNA into the nuclei of living tumor cells. Compared with Lipofectamine 2000 and other investigated gene delivery systems, we were impressed by the rapid and high transfection rate that was displayed by the nano-assembled *c-myc* DNA- Λ -RM0627 system, in addition to its visibility in the nuclei of living cells.

Given these advantages, the developed DNA carrier may provide an invaluable platform for gene delivery applications¹⁷, and could catalyze the fundamental development of a single enantiomer ruthenium (II) complexes as carriers in gene delivery and clinical therapy³. In summary, we developed a novel method by using the a single enantiomer ruthenium (II) complex to promote the self-assembly of the *c-myc* G-quadruplex DNA that could

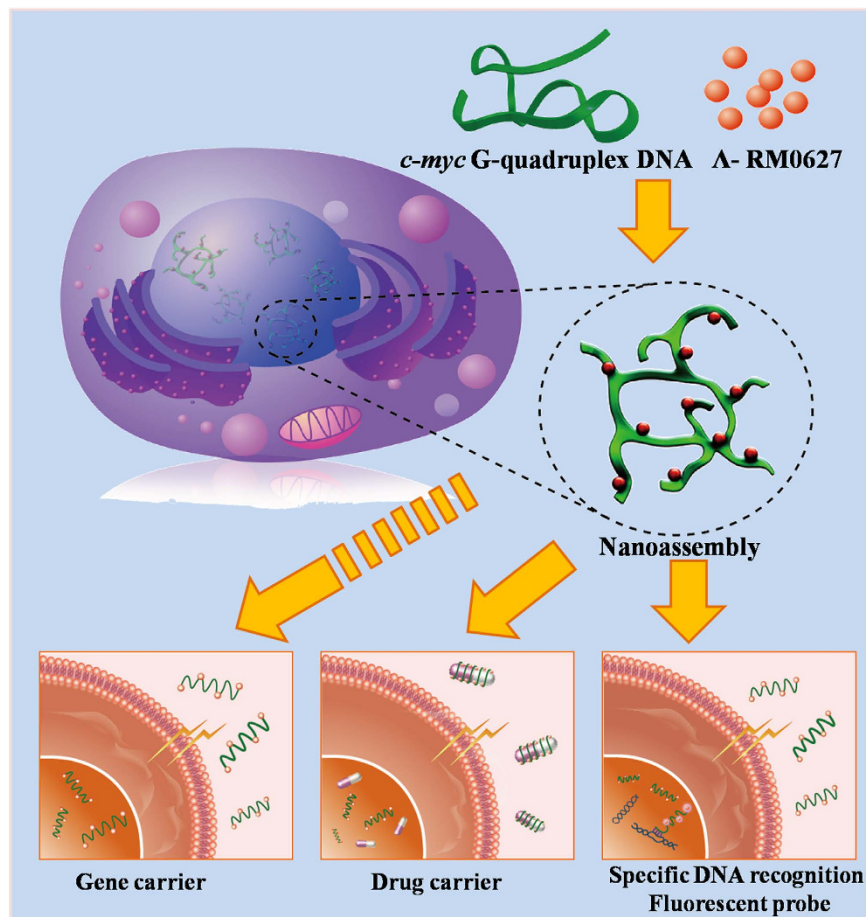


Figure 6. The potential application of the DNA nano-assembly that was promoted by Δ -RM0627. Illustration of the *c-myc* G-quadruplex DNA nano-assembly that was induced by the a single enantiomer ruthenium (II) complex to carry DNA into the nuclei of living cells. Also shown is the potential application of the nano-assembly system as a drug and gene carrier and specific DNA recognizing fluorescent probe.

carry the gene into the nuclei of viable tumor cells. The proposed method could be easily applied to gene therapeutic applications in the near future (Fig. 6).

Methods

Materials. All reagents and solvents were purchased commercially and used without further purification unless specifically noted. Distilled water was used in all experiments. The *c-myc* pu22 DNA (5'-TGGGGAGGGTGGGGAGGGTGGGGAAGG-3') and FITC labelled *c-myc* pu22 DNA (5'-FAM-TGGGGAGGGTGGGGAGGGTGGGGAAGG-3') were purchased from Sangon Biotech (Shanghai) Co., Ltd. The G-quadruplex conformation was formed by denaturation at 90 °C for 5 min followed by denaturation at 4 °C for 24 h, as stipulated by previously published methods⁴³. All aqueous solutions were prepared in double-distilled water. Fetal bovine serum (FBS), Dulbecco's Modified Eagle Medium (DMEM), penicillin and streptomycin were purchased from Gibco/Life Technologies (Grand Island, NY). Hoechst 33258 and DAPI were purchased from Beyotime Biotechnology. Lipofectamine 2000 was purchased from Invitrogen.

Instruments. These complexes were synthesized by using an Anton Paar monowave 300 microwave reactor, which was set at 2450 MHz at an initiating single mode power setting (Biotage). The ¹H NMR, ¹³C NMR and ¹H ¹H COSY spectra were recorded in *d*₆-DMSO solution on a Bruker DRX 2500 spectrometer, and ESI-MS spectra were obtained in methanol on an Agilent 1100 ESI-MS system that was operated at room temperature. UV-vis absorption spectra were recorded on a Shimadzu UV-2550 spectrophotometer using 1 cm path-length quartz cuvettes (3 mL). Circular dichroism (CD) spectra were measured on a Jasco J-810 spectropolarimeter. Cellular localization and real-time fluorescence imaging experiments were measured using an LSCM510 Meta Duo Scan (Carl Zeiss, Germany). The nanostructures were characterized by transmission electron microscopy (TEM, model TECNAI 10) and atomic force microscopy (AFM) (Bruker, Dimension FastScanTM).

Preparation of Δ -RM0627. Δ -RM0627 was synthesized from Δ -[Ru(bpy)₂(*p*-BrPIP)](ClO₄)₂ with phenylacetylene by the Sonogashira coupling reaction, which was followed according to previously published literature but with some modifications⁴⁶.

Self-Assembly of c-myc G-quadruplex DNA with Λ -RM0627. The mixed solution of DNA (50 μ M) and Λ -RM0627 (50 μ M) were incubated for three days, following which the mixed solution at a volume of 100 μ L was added to a copper wire mesh and naturally volatilized for 2 h. An image of the sample was captured by transmission electron microscopy (TEM) using a TECNAI 10 TEM. The mixed solution at a volume of 10 μ L was then removed and added to a mica plate and naturally volatilized for 2 h. Again, an image was captured by atomic force microscopy (AFM) (Bruker, Dimension FastScanTM).

Distribution and location of the nano-assembly of c-myc G-quadruplex DNA with Λ -RM0627. HepG2 cells were cultured in DMEM culture medium that was supplemented with 10% fetal bovine serum (FBS) at 37 °C and 5% CO₂. After being digested by trypsin-EDTA solution, the cells were counted and divided into two parts. Each part (5 × 10⁴ cells) were seeded onto cover slips (18-mm diameter) and allowed to adhere for 12 h before changing the culture medium to DMEM with the nano-assembly of the c-myc G-quadruplex DNA (5 μ M) with Λ -RM0627 (5 μ M). The cells were incubated with the complex for 6 h at 37 °C under 5% CO₂ followed by carefully washing the cells with PBS buffer, then fixed by 4% paraformaldehyde and stained with DAPI. There are no obvious increase membrane permeabilisation under the combination of Λ -RM0627 and laser light in the current laser intensity was observed. The pictures were captured by confocal laser microscopy (Zeiss, LSM 510).

Cellular uptake of the c-myc G-quadruplex DNA nano-assembly with Λ -RM0627 observed in real-time. The HepG2 cells (at a density of 5 × 10⁴ cells) were seeded onto cover slips (18-mm diameter) and allowed to adhere for 12 h. Hoechst 33258 (10 nM) was then added to the living cells and incubated for 30 min to stain the cell nucleus. Next, the culture medium was changed to DMEM solution including the c-myc G-quadruplex DNA (5 μ M) nano-assembly with Λ -RM0627 (5 μ M). Images were then captured by confocal laser microscopy about every 5 min for 150 min.

RT-qPCR analysis. The nanowire system (50 μ M) of Λ -RM0627 and c-myc (sterile KCl Tris-HCl buffer) pre-incubation for 3 days were diluted in DMEM with 10% FBS to 5 μ M. HepG2 cells were incubated with the nanowire system (5 μ M) at 37 °C for 24 h. The primers were purchased from BGI, Trizol was purchased from Invitrogen and quantitative PCR using SYBR green system was purchased from Takara. Total RNA was isolated using Trizol according to the recommendation of the manufacturer. Up to 2 μ g of the total RNA from each sample was reverse transcribed using oligo (dT) primers at 37 °C for 90 min⁴⁷. The relative mRNA levels were evaluated by quantitative PCR using a SYBR green PCR kit. The signals were normalized to β -actin as an internal control. The quantity of c-myc in each BC, relative to the average expression in 40 NATs, was calculated using the following equation: $RQ = 2^{-\Delta\Delta C_T}$, where $\Delta\Delta C_T = (C_{T\text{c-myc}} - C_{T\beta\text{-actin}})_S - (C_{T\text{c-myc}} - C_{T\beta\text{-actin}})_{\text{Mean}_C}$. The primer sequences are listed in the Supporting Information.

References

- Tachibana, M. *et al.* Towards germline gene therapy of inherited mitochondrial diseases. *Nature* **493**, 627–631 (2013).
- Leboulch, P. Gene therapy: primed for take-off. *Nature* **500**, 280–282 (2013).
- Chen, T. *et al.* DNA micelle flares for intracellular mRNA imaging and gene therapy. *Angew. Chem. Int. Ed.* **52**, 2012–2016 (2013).
- Korpisalo, P. *et al.* Capillary enlargement, not sprouting angiogenesis, determines beneficial therapeutic effects and side effects of angiogenic gene therapy. *Eur. Heart J.* **32**, 1664–1672 (2011).
- Yoo, J. Y. *et al.* Tumor suppression by apoptotic and anti-angiogenic effects of mortalin-targeting adeno-oncolytic virus. *J. Gene Med.* **12**, 586–595 (2010).
- Zou, N. *et al.* The hinge of the human papillomavirus type 11 E2 protein contains major determinants for nuclear localization and nuclear matrix association. *J. Virol.* **74**, 3761–3770 (2000).
- Tomecki, R. *et al.* Multiple myeloma-associated hDIS3 mutations cause perturbations in cellular RNA metabolism and suggest hDIS3 PIN domain as a potential drug target. *Nucleic Acids Res.* **42**, 1270–1290 (2014).
- Bald, T. *et al.* Ultraviolet-radiation-induced inflammation promotes angiogenesis and metastasis in melanoma. *Nature* **507**, 109–113 (2014).
- Cianfanelli, V. *et al.* AMBRA1 links autophagy to cell proliferation and tumorigenesis by promoting c-Myc dephosphorylation and degradation. *Nat. Cell Biol.* **17**, 20–30 (2015).
- Nakagawa, M., Takizawa, N., Narita, M., Ichisaka, T. & Yamanaka, S. Promotion of direct reprogramming by transformation-deficient Myc. *Proc. Natl. Acad. Sci.* **107**, 14152–14157 (2010).
- Takayama, N. *et al.* Transient activation of c-MYC expression is critical for efficient platelet generation from human induced pluripotent stem cells. *J. Exp. Med.* **207**, 2817–2830 (2010).
- Ozpolat, B., Sood, A. K. & Lopez-Berestein, G. Nanomedicine based approaches for the delivery of siRNA in cancer. *J. Intern. Med.* **267**, 44–53 (2010).
- Heller, R. & Heller, L. C. Gene electrotransfer clinical trials. *Adv. Genet.* **89**, 235–262 (2015).
- Woltjen, K. *et al.* piggyBac transposition reprograms fibroblasts to induced pluripotent stem cells. *Nature* **458**, 766–770 (2009).
- Montserrat, N. *et al.* Simple generation of human induced pluripotent stem cells using poly-beta-amino esters as the non-viral gene delivery system. *J. Biol. Chem.* **286**, 12417–12428 (2011).
- Huo, S. *et al.* Ultrasmall gold nanoparticles as carriers for nucleus-based gene therapy due to size-dependent nuclear entry. *ACS Nano* **8**, 5852–5862 (2014).
- Liu, L. *et al.* Dinuclear metal(II) complexes of polybenzimidazole ligands as carriers for DNA delivery. *Biomaterials* **31**, 1380–1391 (2010).
- Jiang, R. W., Yin, J., Hu, S., Meng, X. G. & Liu, C. L. Cobalt(II)-Polybenzimidazole Complexes as a Nonviral Gene Carrier: Effects of Charges and Benzimidazolyl Groups. *Curr. Drug Deliv.* **10**, 122–133 (2013).
- Liu, Y. *et al.* A luminescent beta-cyclodextrin-based Ru(phen)₃ complex as DNA compactor, enzyme inhibitor, and translocation tracer. *ACS Nano* **1**, 313–318 (2007).
- Sun, B. *et al.* DNA Condensation Induced by Ruthenium(II) Polypyridyl Complexes [Ru(bpy)₂(PIPSh)]²⁺ and [Ru(bpy)₂(PIPNH)]²⁺. *Inorg. Chemistry* **48**, 4637–4639 (2009).
- Bhat, S. S. *et al.* Ruthenium(II) polypyridyl complexes as carriers for DNA delivery. *Chem. Commun.* **47**, 11068–11070 (2011).
- Yu, B. L. *et al.* A luminescent tetranuclear ruthenium(II) complex as a tracking non-viral gene vector. *Chem. Commun.* **49**, 810–812 (2013).

23. Qiu, K. *et al.* Tetranuclear ruthenium(II) complexes with oligo-oxyethylene linkers as one- and two-photon luminescent tracking non-viral gene vectors. *Dalton Trans.* **44**, 7058–7065 (2015).
24. Yu, B. L. *et al.* Lipophilic Tetranuclear Ruthenium(II) Complexes as Two-Photon Luminescent Tracking Non-Viral Gene Vectors. *Sci. Rep.* **5**, 10707 (2015)
25. Yu, B. L. *et al.* Lipophilic Tetranuclear Ruthenium(II) Complexes as Two-Photon Luminescent Tracking Non-Viral Gene Vectors. *Chem. Eur. J.* **21**, 3691–3700 (2015).
26. Xu, L. *et al.* Dinuclear Ruthenium(II) Complexes That Induce and Stabilise G-Quadruplex DNA. *Chem. Eur. J.* **21**, 4008–4020 (2015).
27. Liao, G. L., Chen, X., Ji, L. N. & Chao, H. Visual specific luminescent probing of hybrid G-quadruplex DNA by a ruthenium polypyridyl complex. *Chem. Commun. (Camb)* **48**, 10781–10783 (2012).
28. Wang, J., Chen, Y., Ren, J., Zhao, C. & Qu, X. G-Quadruplex binding enantiomers show a single enantiomer selective interactions with human telomere. *Nucleic Acids Res.* **42**, 3792–3802 (2014).
29. Wang, K. *et al.* Self-assembly of a bifunctional DNA carrier for drug delivery. *Angew. Chem. Int. Ed.* **50**, 6098–6101 (2011).
30. Huang, F. *et al.* Self-assembled hybrid nanoparticles for targeted co-delivery of two drugs into cancer cells. *Chem. Commun. (Camb)* **50**, 3103–3105 (2014).
31. Wang, J. *et al.* BaHoF5 nanopores as high-performance contrast agents for multi-modal CT imaging of ischemic stroke. *Biomaterials* **71**, 110–118 (2015).
32. Murat, P., Singh, Y. & DeFrancq, E. Methods for investigating G-quadruplex DNA/ligand interactions. *Chem. Soc. Rev.* **40**, 5293–5307 (2011).
33. You, H., Wu, J., Shao, F. & Yan, J. Stability and kinetics of c-MYC promoter G-quadruplexes studied by single-molecule manipulation. *J. Am. Chem. Soc.* **137**, 2424–2427 (2015).
34. Wu, Q. *et al.* Microwave-assisted synthesis of arene ruthenium(II) complexes [(eta(6)-RC6H5)Ru(m-MOPIP)Cl]Cl (R = -H and -CH3) as groove binder to c-myc G4 DNA. *Dalton Trans.* **43**, 9216–9225 (2014).
35. Zhang, Z. *et al.* Ruthenium(II) complexes as apoptosis inducers by stabilizing c-myc G-quadruplex DNA. *Eur. J. Med. Chem.* **80**, 316–324 (2014).
36. Catherall, T., Huskisson, D., McAdams, S. & Vijayaraghavan, A. Self-assembly of one dimensional DNA-templated structures. *J. Mat. Chem. C* **2**, 6895–6920 (2014).
37. Yatsunyk, L. A. *et al.* Guided assembly of tetramolecular G-quadruplexes. *ACS Nano* **7**, 5701–5710 (2013).
38. Hessari, N. M. *et al.* Programmed self-assembly of a quadruplex DNA nanowire. *Eur. J. Chem.* **20**, 3626–3630 (2014).
39. Rudiuk, S., Venancio-Marques, A., Hallais, G. & Baigl, D. Preparation of one- to four-branch silver nanostructures of various sizes by metallization of hybrid DNA-protein assemblies. *Soft Mat.* **9**, 9146–9152 (2013).
40. Baggaley, E. *et al.* Dinuclear ruthenium(II) complexes as two-photon, time-resolved emission microscopy probes for cellular DNA. *Angew. Chem. Int. Ed.* **53**, 3367–3371 (2014).
41. Gill, M. R. *et al.* A ruthenium(II) polypyridyl complex for direct imaging of DNA structure in living cells. *Nat. Chem.* **1**, 662–667 (2009).
42. Lai, Y. T. *et al.* Rapid labeling of intracellular His-tagged proteins in living cells. *Proc. Natl. Acad. Sci.* **112**, 2948–2953 (2015).
43. Hu, R. *et al.* DNA nanoflowers for multiplexed cellular imaging and traceable targeted drug delivery. *Angew. Chem. Int. Ed.* **53**, 5821–5826 (2014).
44. Fiszer-Kierzkowska, A. *et al.* Liposome-based DNA carriers may induce cellular stress response and change gene expression pattern in transfected cells. *BMC Mol. Biol.* **12**, 27 (2011).
45. Ou, T. M. *et al.* Stabilization of G-quadruplex DNA and down-regulation of oncogene c-myc by quindoline derivatives. *J. Med. Chem.* **50**, 1465–1474 (2007).
46. Zhong, H., Wang, J., Li, L. & Wang, R. The copper-free Sonogashira cross-coupling reaction promoted by palladium complexes of nitrogen-containing chelating ligands in neat water at room temperature. *Dalton Trans.* **43**, 2098–2103 (2014).
47. Zhang, Y. *et al.* Sp1 and c-Myc modulate drug resistance of leukemia stem cells by regulating survivin expression through the ERK-MSK MAPK signaling pathway. *Mol. Cancer* **14**, 56 (2015).

Acknowledgements

The authors acknowledge the National Nature Science Foundation of China (Grant Number: 81572926), the Provincial Major Scientific Research Projects in Universities of Guangdong Province (Grant Number: 2014KZDXM053), the Science and Technology Project of Guangdong Province (Grant Number: 2014A020212312), the Guangzhou City Science and Technology Plan (Grant Number: 2013J4100072), the Science and Technology Projects of Yuexiu District (Grant Number: 2014-WS-039), and the Joint Natural Sciences Fund of the Department of Science and Technology and the First Affiliated Hospital of Guangdong Pharmaceutical University (Grant Number: GYFYLH201309).

Author Contributions

Q.W. performed the experiments including TEM and AFM characterization of the DNA nano-assembly and the analysis of the results, and provided Confocal laser scanning microscopy to observe the uptake of the DNA nano-assembly into HepG2 cells, as well as RT-qPCR analysis of the release and expression of the c-myc gene, and wrote and revised the manuscript. Q.W. prepared Figures 1–5. W.M. provided the funds, guided the research, performed the main experiments of preparing the ruthenium complex Λ -RM0627, and obtained the characterization results of Λ -RM0627, and wrote and revised the manuscript. W.M. prepared Figure 6. K.-D.Z. performed the experiments of preparing the chemical intermediate Λ -[Ru(bpy)₂(p-BrPIP)](ClO₄)₂ and p-BrPIP. Yang Ding performed the MTT assay of Λ -RM0627 and the nano-assembly.

Additional Information

Supplementary information accompanies this paper at <http://www.nature.com/srep>

Competing financial interests: The authors declare no competing financial interests.

How to cite this article: Wu, Q. *et al.* Self-assembly of c-myc DNA promoted by a single enantiomer ruthenium complex as a potential nuclear targeting gene carrier. *Sci. Rep.* **6**, 28582; doi: 10.1038/srep28582 (2016).



This work is licensed under a Creative Commons Attribution 4.0 International License. The images or other third party material in this article are included in the article's Creative Commons license, unless indicated otherwise in the credit line; if the material is not included under the Creative Commons license, users will need to obtain permission from the license holder to reproduce the material. To view a copy of this license, visit <http://creativecommons.org/licenses/by/4.0/>